entropy

MDPI

Article

Detecting Initial System–Environment Correlations from a Single Observable: Theory, Performance, and Applications

Ali Abu-Nada [1,*], Russell R. Ceballos [2,3] and Lian-Ao Wu [4,5,6]

[1] General Education Department, Sharjah Maritime Academy, Khor Fakkan P.O. Box 180018, United Arab Emirates
[2] Department of Physical Sciences, Olive-Harvey College, City Colleges of Chicago, 10001 S Woodlawn Ave., Chicago, IL 60628, USA; rceballos@qusteam.org
[3] QuSTEAM Initiative, 510 Ronalds St., Iowa City, IA 52245, USA
[4] Department of Physics, University of the Basque Country UPV/EHU, 48080 Bilbao, Spain; lianaowu@gmail.com
[5] IKERBASQUE, Basque Foundation for Science, 48011 Bilbao, Spain
[6] EHU Quantum Center, University of the Basque Country UPV/EHU, 48940 Leioa, Spain
* Correspondence: ali.abunada@sma.ac.ae

Abstract

Initial correlations between a quantum system and its environment can strongly influence open-system dynamics and invalidate standard reduced-dynamics descriptions. Detecting such correlations is therefore an important problem, but most existing approaches require state tomography, multiple system preparations, or some degree of access to the environment. Here we show that initial system–environment correlations can be certified using only a single calibrated system observable when the interaction is known. For a qubit interacting with an environment via isotropic Heisenberg exchange, we derive exact bounds on the signal $z(t) = \langle \sigma_z^S \rangle(t)$ that hold for all factorized initial states sharing the same calibrated reduced system state. These bounds define a *factorized envelope*: if an observed trajectory exits this envelope, initial correlations are unambiguously certified. The witness requires only single-axis measurements after a one-time calibration of $\rho_S(0)$ and does not rely on environment access or state tomography. We illustrate the method for several families of correlated initial states and show that the same single-observable logic extends to an exactly solvable pure-dephasing spin–boson model with an infinite environment.

Keywords: open quantum systems; initial system–environment correlations; Heisenberg exchange interaction; quantum correlations; correlation witness; single-observable detection

1. Introduction

A controllable quantum system is never perfectly isolated. In realistic settings it interacts with surrounding degrees of freedom that are not directly accessible and are therefore treated as an environment [1,2]. This coupling gives rise to open-system dynamics, whose behavior may depend not only on noise generated during the evolution but also on correlations that are already present between the system and the environment at the initial time [3–7]. Such initial system–environment correlations are of fundamental interest because they can invalidate the standard assumption that reduced dynamics are generated by a completely positive map defined on the full system state space [3–5]. They are also operationally important because they can mimic or mask genuine memory effects: for example, revivals in state distinguishability may originate from correlations already present at $t = 0$ rather than from information backflow generated during the subsequent evolution [6,7].

Check for updates

Academic Editor: Changshui Yu

Received: 29 June 2026
Revised: 19 July 2026
Accepted: 22 July 2026
Published: 24 July 2026

Copyright: © 2026 by the authors. Licensee MDPI, Basel, Switzerland. This article is an open access article distributed under the terms and conditions of the Creative Commons Attribution (CC BY) license.

At the same time, initial system–environment correlations are not merely a nuisance. When deliberately engineered, they can serve as a resource and modify the effective action of environmental noise in useful ways. In particular, appropriately structured initial system–environment entanglement can in some settings suppress decoherence or improve the robustness of quantum information processing (see Ref. [8]). Whether detrimental or beneficial, however, such correlations must first be identified. This makes the detection of initial system–environment correlations a central problem in the theory and practice of open quantum systems.

If both the system and the environment were experimentally accessible, one could in principle detect correlations by joint measurements or full tomography of the combined state [7,9]. In most physical platforms, however, direct access to environmental degrees of freedom is either limited or completely absent. This raises a basic and practically important question:

> *To what extent can initial system–environment correlations be detected using measurements on the system alone?*

A number of system-only strategies have been developed. Some methods compare the dynamics generated by multiple initial system preparations and infer correlations by testing whether the effective environment state depends on the chosen preparation [7,10]. Others use trace distance or related distinguishability measures between reduced system states, where an increase in distinguishability can witness either initial correlations or non-Markovian behavior [6,11–16]. These approaches are powerful and conceptually important, but they typically require either many initial preparations or some form of reduced-state tomography. Even when the environment is never measured, the experimentalist often still needs to reconstruct the full Bloch vector of the system by measuring several noncommuting observables.

A complementary line of work assumes prior knowledge of the joint dynamics. When the interaction Hamiltonian is known, one can ask whether an observed reduced evolution is compatible with any factorized initial state of the form $\rho_S(0) \otimes \rho_E(0)$ [17,18]. Recent theoretical results have shown that, under broad conditions, initial correlations are in principle always detectable from system-only data provided the joint dynamics are known and suitable measurements are performed [19]. Experimentally, system-only detection of initial entanglement with an inaccessible environment has also been demonstrated without full two-qubit tomography, by exploiting prior knowledge of the interaction model [20]. These results strongly support the view that initial correlations can be detected without direct environment access.

Despite this progress, most existing protocols still rely on reconstructing the reduced state of the system, or at least on measuring more than one observable. In many experimentally relevant settings—including NMR platforms, trapped ions, superconducting circuits, and NV centers—this tomographic overhead is nontrivial [6,7,9,11,15,21,22]. This motivates a sharper question than the one usually asked:

> *Can initial system–environment correlations be certified using only a single expectation value of a single system observable, measured along one fixed axis?*

In this work we answer this question affirmatively for a paradigmatic and exactly solvable model. We consider a qubit system interacting with a qubit environment through the isotropic Heisenberg exchange Hamiltonian and assume that the initial reduced state $\rho_S(0)$ is calibrated once at the beginning of the protocol. After this one-time calibration, no further tomography is performed. Instead, we monitor only the single signal $z(t) = \langle \sigma_z^S \rangle(t)$, obtained from repeated measurements of σ_z^S at different evolution times. We ask which

trajectories of this single observable are compatible with *all* factorized initial states that share the same calibrated reduced state.

Our central result is that, for the isotropic Heisenberg exchange, all such factorized initial states generate a closed and exactly computable time-dependent interval $\mathcal{R}(t) = [z_{\min}(t), z_{\max}(t)]$, which we call the *factorized envelope*. This envelope contains every trajectory $z(t)$ obtainable from an uncorrelated preparation consistent with the same $\rho_S(0)$. Consequently, if an experimentally observed trajectory leaves this envelope at any time, then no product initial state can explain the data, and initial system–environment correlations are certified. The witness is one-sided, analytically exact, and experimentally economical: after the initial calibration, it requires only repeated measurements of a single observable along a fixed axis.

It is important to emphasize, however, that the witness is inherently one-sided. While any violation of the factorized envelope provides an unambiguous certification of initial system–environment correlations, the converse does not hold. A trajectory that remains entirely inside the envelope is still compatible with correlated initial states and therefore cannot be interpreted as evidence that the initial state was uncorrelated.

It is important to emphasize that the proposed witness is inherently one-sided. If an experimentally observed trajectory leaves the factorized envelope, then no factorized initial state sharing the same calibrated reduced system state can reproduce the observation, and initial system–environment correlations are therefore certified. Conversely, a trajectory that remains entirely within the envelope does not establish that the initial state was factorized, since correlated initial states may still generate trajectories compatible with the factorized null hypothesis.

From the perspective of reduced dynamics, the construction has a natural operational interpretation. When initial correlations may be present, the reduced evolution depends on how the reduced input state is embedded into the joint system–environment space, a dependence commonly described in terms of assignment (embedding) maps [3–5]. In our setting, the standard product assignment $\mathcal{A}_{\mathrm{prod}}(\rho_S) = \rho_S \otimes \rho_E$ serves as a null hypothesis for uncorrelated preparations. The factorized envelope is then precisely the admissible region generated by this product embedding. A measured violation of the envelope therefore rules out the entire product-assignment class using only a single calibrated observable, without reconstructing $\rho_S(t)$ at later times and without inferring a general assignment map from data.

The isotropic Heisenberg exchange model is particularly suitable for this program because it admits both an exact analytic treatment and a transparent geometric interpretation. For factorized initial states, the reduced Bloch vector follows a structured partial-swap trajectory between the system and environment Bloch vectors. This makes it possible to characterize the admissible single-observable dynamics in closed form and to visualize the witness geometrically. We show that the resulting envelope can be violated by several families of correlated initial states, including cases in which the reduced system state is maximally mixed and therefore carries no direct signature of the hidden correlations at $t = 0$.

Although the isotropic Heisenberg exchange interaction serves as our primary example, the proposed framework is not conceptually restricted to this specific model. The Heisenberg Hamiltonian was chosen because it is a paradigmatic interaction in quantum information science and condensed-matter physics and, importantly, admits an exact analytical characterization of the factorized compatibility envelope. The essential ingredient of our approach is the availability of a sufficiently characterized interaction Hamiltonian that allows the admissible single-observable dynamics generated by all factorized initial states to be determined. Consequently, the same compatibility-based philosophy may be extended to broader classes of system–environment interactions whenever analogous

analytical or numerical characterizations are available. Investigating such extensions, including anisotropic exchange models and other exactly solvable open-system Hamiltonians, represents an important direction for future work.

Although our main development uses a minimal two-qubit model, the underlying idea is more general. To demonstrate that the witness is not an artifact of a finite-dimensional environment, we also extend the same single-observable logic to an exactly solvable pure-dephasing spin–boson model with an infinite bath. In that setting, factorized initial states again generate a sharply constrained admissible region for a single system observable, and violations of that region certify initial correlations.

The present protocol assumes that the system–environment interaction Hamiltonian has been independently characterized through prior experimental calibration. We emphasize that this assumption defines the intended scope of the method rather than a universal description of all open quantum systems. While it may be restrictive for complex molecular or condensed-matter environments, where microscopic interactions are often only approximately known, it is well justified for many engineered quantum platforms—including superconducting circuits, trapped ions, semiconductor spin qubits, and NV centers—where effective interaction Hamiltonians are routinely identified and calibrated before experiments are performed. Extending the present compatibility-based framework to partially characterized or uncertain interaction models remains an important direction for future research.

The present work differs from previous tomography-free and reduced-resource approaches in both its null hypothesis and its measurement requirements. Existing system-only methods commonly infer initial correlations by comparing several reduced trajectories, preparing multiple initial system states, monitoring distinguishability measures, or reconstructing part or all of the reduced density operator. In contrast, we fix a single calibrated reduced system state and determine the complete range of one fixed observable that can be generated by every factorized initial state compatible with that calibration. The resulting factorized-envelope construction therefore provides an exact single-observable compatibility test rather than a reconstruction-based criterion.

The novelty of the present work lies in the combination of several elements: an analytically exact factorized envelope, optimization over all unknown environment qubit states, measurements along only one fixed axis after a one-time calibration, a geometric partial-SWAP interpretation, and an assignment-map formulation in which the product embedding serves as the factorized null hypothesis. Reference [23], whose state families are used in Section 6, did not derive the single-observable factorized envelope or the associated certification theorem developed here. We additionally examine how the same compatibility-based reasoning may be implemented in a characterized infinite-dimensional pure-dephasing environment. More broadly, methods originating from open quantum-system theory and quantum-inspired dynamical models have also found applications in the description of complex systems beyond traditional physics, including network dynamics and social processes [24].

The main contributions of this work are therefore fourfold. First, we derive an analytically exact factorized compatibility envelope for a single system observable under isotropic Heisenberg exchange by optimizing over all environment qubit states. Second, after a one-time calibration of the reduced initial system state, the protocol requires measurements along only one fixed system axis, without reduced-state tomography during the evolution or direct access to the environment. Third, we provide both a geometric partial-SWAP interpretation and an assignment-map formulation of the factorized null hypothesis. Fourth, we investigate how the same compatibility principle can be applied to a characterized pure-dephasing spin–boson model with an infinite-dimensional environment.

In contrast to previous tomography-free approaches, the present work derives an exact factorized compatibility envelope for a single calibrated observable, provides a closed-form analytical construction under isotropic Heisenberg exchange, develops a geometric interpretation of the witness, formulates the protocol within the assignment-map framework, and demonstrates its extension to an exactly solvable infinite-dimensional model.

The remainder of the paper is organized as follows. Section 2 describes the operational protocol. Section 3 introduces the model and notation. Section 4 derives the factorized envelope. Section 6 presents illustrative examples. Section 7 extends the approach to the pure-dephasing spin–boson model. Finally, we conclude with a discussion.

2. Procedure

In this section we describe the protocol in an operational manner, emphasizing how it is implemented in practice and how the resulting data are interpreted. We clearly separate what is done *in the laboratory* from what is done *in theory* to interpret the experimental data.

2.1. What Is the Basic Idea?

When a quantum system interacts with an environment, correlations can appear in two different ways:

- Correlations can be *created during the evolution*, even if the system and environment were initially uncorrelated;
- Correlations can already *exist at the initial time*, before the evolution begins.

In this work we focus on the second case: *how can we tell whether correlations were already present at the initial time, using measurements on the system only?*

We assume that the interaction Hamiltonian H is known, and that the initial state of the system $\rho_S(0)$ can be calibrated once. After that, we only measure a single observable of the system, $z(t) = \langle \sigma_z^S \rangle(t)$.

The key question is therefore:

Given the calibrated system state $\rho_S(0)$ and a known interaction H, which values of $z(t)$ are possible if the initial state was uncorrelated?

If we can determine this range, then any experimentally observed value outside it proves that the initial state must have been correlated.

For the isotropic Heisenberg exchange, we show that all uncorrelated (product) initial states lead to values of $z(t)$ inside a time-dependent interval,

$$\mathcal{R}(t) = [z_{\min}(t), z_{\max}(t)], \tag{1}$$

which we call the *factorized envelope*.

2.2. Experimental Protocol (Steps 1–3)

The first three steps describe only what the experimentalist does in the laboratory. At this stage, no assumption is made about whether the system and environment are correlated.

Step 1: Calibrate the system state

Prepare the system qubit S in a known reduced state,

$$\rho_S(0) = \tfrac{1}{2}\left(\mathbb{I} + \vec{s} \cdot \vec{\sigma}\right), \tag{2}$$

where $\vec{s} = (s_x, s_y, s_z)$ is the Bloch vector. The vector $\vec{s}$ is determined in a separate calibration run, for example by performing tomography at time $t = 0$.

This calibration is done only once. Afterward, no further tomography is required. The environment E starts in some unknown state $\rho_E(0)$, which may or may not be correlated with the system.

Step 2: Let the system and environment interact

In each run of the experiment, the joint system starts in some physical state $\rho_{SE}(0)$ whose system marginal is the calibrated $\rho_S(0)$. The joint evolution is governed by the known Hamiltonian H,

$$\rho_{SE}(t) = U(t)\,\rho_{SE}(0)\,U^\dagger(t), \qquad U(t) = e^{-iHt}. \tag{3}$$

Operationally, the experimentalist simply prepares the same initial state as reproducibly as possible and allows the system and environment to interact for a time t.

Step 3: Measure a single observable

For a chosen evolution time t, the experiment is repeated many times:

1. Prepare the same initial joint state;
2. Let it evolve for time t;
3. Measure σ_z^S on the system.

Averaging the measurement outcomes gives

$$z(t) = \langle \sigma_z^S \rangle(t) = \mathrm{Tr}_S[\rho_S(t)\,\sigma_z^S], \tag{4}$$

where $\rho_S(t) = \mathrm{Tr}_E[\rho_{SE}(t)]$. Only this single observable is measured, and the measurement axis is fixed throughout the experiment.

2.3. Theoretical Analysis (Steps 4–5)

We now explain how the experimental data are interpreted.

Step 4: Define the uncorrelated reference model

To test whether the data are compatible with an uncorrelated preparation, we introduce a *theoretical null hypothesis*. We assume that the initial joint state is uncorrelated and given by $\rho_{SE}(0) = \rho_S(0) \otimes \rho_E(0)$, where $\rho_E(0)$ is arbitrary.

This assumption corresponds to the standard *product assignment map*, which embeds the calibrated system state into a joint state assuming no initial correlations.

Under this assumption, different environment states lead to different trajectories $z(t)$. The set of all values obtainable in this way defines the factorized envelope,

$$\mathcal{R}(t) = \left\{ z(t) \;\middle|\; \rho_{SE}(0) = \rho_S(0) \otimes \rho_E(0) \right\} = [z_{\min}(t), z_{\max}(t)]. \tag{5}$$

For the isotropic Heisenberg exchange, the bounds $z_{\min}(t)$ and $z_{\max}(t)$ can be computed analytically as shown in Section 4.

Step 5: Compare theory and experiment

Finally, the experimentally measured value $\tilde{z}(t)$ is compared with the theoretical interval $\mathcal{R}(t)$. If for some time t^* one finds

$$\tilde{z}(t^*) \notin \mathcal{R}(t^*)$$

then no uncorrelated (product) initial state can explain the observation. This certifies the presence of initial system–environment correlations.

Figure 1 provides a schematic illustration of the factorized envelope and how an experimentally observed trajectory can certify initial correlations by exiting this admissible region.

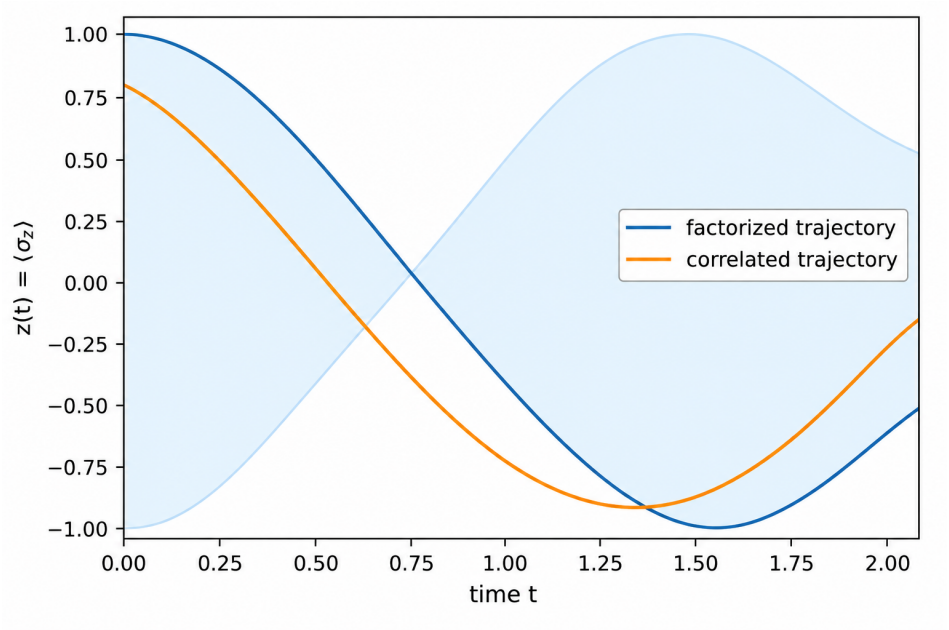


Figure 1. Illustration of the factorized-envelope witness. The shaded region represents the factorized envelope $\mathcal{R}(t) = [z_{\min}(t), z_{\max}(t)]$, containing all trajectories $z(t) = \langle \sigma_z^S \rangle(t)$ obtainable from factorized initial states $\rho_{SE}(0) = \rho_S(0) \otimes \rho_E(0)$. The blue curve shows a representative factorized trajectory lying entirely inside the envelope, while the orange curve corresponds to a correlated initial state that exits the envelope, thereby certifying initial system–environment correlations.

3. Model and Definitions

We now formalize the setting and notation.

We consider a system qubit S and an environment qubit E with joint Hilbert space

$$\mathcal{H}_{SE} = \mathcal{H}_S \otimes \mathcal{H}_E, \qquad \dim \mathcal{H}_S = \dim \mathcal{H}_E = 2. \tag{6}$$

The initial joint state $\rho_{SE}(0)$ may be either

$$\rho_{SE}(0) = \rho_S(0) \otimes \rho_E(0) \quad \text{(factorized)}, \tag{7}$$

or

$$\rho_{SE}(0) \neq \rho_S(0) \otimes \rho_E(0) \quad \text{(correlated)}, \tag{8}$$

where the latter may contain classical and/or quantum correlations, including entanglement.

The joint evolution is generated by a known Hamiltonian H on $\mathcal{H}_{SE}$, with unitary $U(t) = e^{-iHt}$ and

$$\rho_{SE}(t) = U(t)\rho_{SE}(0)U^\dagger(t). \tag{9}$$

The reduced state of the system is

$$\rho_S(t) = \mathrm{Tr}_E[\rho_{SE}(t)]. \tag{10}$$

The calibrated initial state of S is written in Bloch form as

$$\rho_S(0) = \tfrac{1}{2}\big(\mathbb{I} + \vec{s} \cdot \vec{\sigma}\big), \qquad |\vec{s}| \leq 1, \tag{11}$$

where $\vec{\sigma} = (\sigma_x, \sigma_y, \sigma_z)$ is the Pauli vector and $\vec{s} \in \mathbb{R}^3$ is the initial Bloch vector. At time t the reduced state is

$$\rho_S(t) = \tfrac{1}{2}\big(\mathbb{I} + \vec{s}(t) \cdot \vec{\sigma}\big), \qquad |\vec{s}(t)| \leq 1, \tag{12}$$

with Bloch vector $\vec{s}(t) = (s_x(t), s_y(t), s_z(t))$.

The quantity accessible in our protocol is the single expectation value.

The measured signal can be written equivalently in the Schrödinger and Heisenberg pictures as

$$\begin{aligned} z(t) &= \left\langle \sigma_z^S \right\rangle_t \\ &= \mathrm{Tr}_S\left[\rho_S(t)\sigma_z^S\right] \\ &= \mathrm{Tr}_{SE}\left[\rho_{SE}(0)U^\dagger(t)\left(\sigma_z^S \otimes \mathbb{I}_E\right)U(t)\right]. \end{aligned} \tag{13}$$

Equivalently, defining the Heisenberg-picture joint observable

$$\sigma_z^S(t) = U^\dagger(t)\left(\sigma_z^S \otimes \mathbb{I}_E\right)U(t), \tag{14}$$

we have

$$z(t) = \mathrm{Tr}_{SE}\left[\rho_{SE}(0)\sigma_z^S(t)\right]. \tag{15}$$

When the initial state is factorized, we may write the environment as

$$\rho_E(0) = \tfrac{1}{2}\left(\mathbb{I} + \vec{e}\cdot\vec{\sigma}\right), \qquad |\vec{e}| \le 1, \tag{16}$$

but in the protocol we never need to know $\vec{e}$ explicitly.

For each fixed t we define the set of all values of $z(t)$ obtainable from factorized initial states with the given calibration:

$$\mathcal{R}(t) = \left\{\, z(t) \;\middle|\; \rho_{SE}(0) = \rho_S(0) \otimes \rho_E(0) \,\right\}. \tag{17}$$

Our main technical goal is to compute $\mathcal{R}(t)$ explicitly for the isotropic exchange Hamiltonian and to show that it is always an interval

$$\mathcal{R}(t) = [\, z_{\min}(t), z_{\max}(t) \,]. \tag{18}$$

Explicit formulas for $z_{\min}(t)$ and $z_{\max}(t)$ are obtained in Section 4.

Reduced-Dynamics Viewpoint: Assignment Maps and the Product Admissible Set

A reduced system trajectory is ultimately generated by a joint unitary evolution on SE followed by a partial trace. When initial correlations may be present, a key foundational issue is that the reduced evolution cannot, in general, be represented by a single completely positive (CP) map on the full system state space without additional physical structure; instead, one must specify how a given reduced state $\rho_S(0)$ is embedded into the joint space. This is naturally captured by an *assignment map* (or embedding) $\mathcal{A}$, which assigns to each reduced input state a compatible joint state,

$$\rho_{SE}(0) = \mathcal{A}\big(\rho_S(0)\big), \tag{19}$$

and generates the reduced dynamics

$$\rho_S(t) = \mathrm{Tr}_E\Big[U(t)\,\mathcal{A}\big(\rho_S(0)\big)\,U^\dagger(t)\Big]. \tag{20}$$

In general, $\mathcal{A}$ need not be unique, and physical consistency requirements may restrict the *domain* on which a given reduced description is valid. A useful structural condition is *G-consistency*: for a specified set of allowed global unitaries G, different joint states that

share the same reduced state must induce the same reduced evolution under all $U \in G$, ensuring that the reduced dynamics are well defined on the chosen domain (see Ref. [25]).

In our protocol, we do *not* attempt to reconstruct $\rho_S(t)$ or infer $\mathcal{A}$ in full generality. Instead, we fix the reduced input state $\rho_S(0)$ once by calibration and monitor only the single expectation value

$$z(t) = \mathrm{Tr}_S\big[\rho_S(t)\,\sigma_z^S\big] = \mathrm{Tr}_{SE}\big[\mathcal{A}\big(\rho_S(0)\big)\,U^\dagger(t)(\sigma_z^S \otimes \mathbb{I})U(t)\big]. \tag{21}$$

This viewpoint makes clear that even without full tomography, one can define a sharp *compatibility set* for factorized preparations by restricting to the standard product assignment

$$\mathcal{A}_{\mathrm{prod}}\big(\rho_S(0)\big) = \rho_S(0) \otimes \rho_E(0), \tag{22}$$

with arbitrary environment state $\rho_E(0)$. For fixed $\rho_S(0)$ and t, the set of all values of $z(t)$ obtainable from (22) is exactly the factorized admissible region,

$$\mathcal{R}(t) = \Big\{ z(t) \;\Big|\; \rho_{SE}(0) = \rho_S(0) \otimes \rho_E(0) \Big\}. \tag{23}$$

Because $z(t)$ is affine in the unknown environment parameters under the product assignment, $\mathcal{R}(t)$ is an interval $[z_{\min}(t), z_{\max}(t)]$ whose endpoints are achieved by pure environment states. If an observed trajectory leaves this interval at any time, then no product assignment (22) can explain the data, and the initial joint state must have contained correlations. In Section 4 we compute $z_{\min\,/\,\max}(t)$ analytically for the isotropic Heisenberg exchange.

4. Heisenberg Exchange Dynamics and Envelope

We now specialize to the isotropic Heisenberg exchange Hamiltonian

$$H_{\mathrm{ex}} = J\big(\sigma_x^S\sigma_x^E + \sigma_y^S\sigma_y^E + \sigma_z^S\sigma_z^E\big) = J\,\vec{\sigma}_S \cdot \vec{\sigma}_E, \tag{24}$$

with factorized initial state

$$\rho_{SE}(0) = \rho_S \otimes \rho_E, \quad \rho_S = \tfrac{1}{2}(\mathbb{I} + \vec{s}\cdot\vec{\sigma}), \quad \rho_E = \tfrac{1}{2}(\mathbb{I} + \vec{e}\cdot\vec{\sigma}). \tag{25}$$

Proposition 1. *Let the system and environment be two qubits evolving under the isotropic exchange Hamiltonian*

$$H_{\mathrm{ex}} = J\,\vec{\sigma}_S \cdot \vec{\sigma}_E. \tag{26}$$

Assume that the initial state is factorized,

$$\rho_{SE}(0) = \rho_S \otimes \rho_E, \tag{27}$$

where

$$\rho_S = \frac{1}{2}(\mathbb{I} + \vec{s}\cdot\vec{\sigma}), \qquad \rho_E = \frac{1}{2}(\mathbb{I} + \vec{e}\cdot\vec{\sigma}). \tag{28}$$

Then the reduced system state at time t is

$$\rho_S(t) = \frac{1}{2}[\mathbb{I} + \vec{s}(t)\cdot\vec{\sigma}], \tag{29}$$

with Bloch vector

$$\vec{s}(t) = c^2\vec{s} + d^2\vec{e} - cd\,(\vec{s}\times\vec{e}) \tag{30}$$

where

$$c = \cos(2Jt), \qquad d = \sin(2Jt). \tag{31}$$

Proof. Introduce the SWAP operator

$$S = \frac{1}{2}(\mathbb{I} + \vec{\sigma}_S \cdot \vec{\sigma}_E). \tag{32}$$

This operator satisfies

$$S^2 = \mathbb{I}, \tag{33}$$

and exchanges the two qubits according to

$$S(A \otimes B)S = B \otimes A. \tag{34}$$

From the definition of S, we have

$$2S = \mathbb{I} + \vec{\sigma}_S \cdot \vec{\sigma}_E. \tag{35}$$

Therefore

$$\vec{\sigma}_S \cdot \vec{\sigma}_E = 2S - \mathbb{I}. \tag{36}$$

Hence the Hamiltonian can be written as

$$H_{\text{ex}} = J(2S - \mathbb{I}). \tag{37}$$

The unitary evolution operator is then

$$\begin{aligned} U(t) &= e^{-iH_{\text{ex}}t} \\ &= e^{-iJ(2S-\mathbb{I})t} \\ &= e^{iJt}e^{-i2JtS}. \end{aligned} \tag{38}$$

Since $S^2 = \mathbb{I}$, we obtain

$$e^{-i2JtS} = \cos(2Jt)\mathbb{I} - i\sin(2Jt)S. \tag{39}$$

The global phase e^{iJt} cancels in $U(t)\rho_{SE}(0)U^\dagger(t)$, so it may be omitted. Thus we write

$$U(t) = c\mathbb{I} - idS, \tag{40}$$

where

$$c = \cos(2Jt), \qquad d = \sin(2Jt). \tag{41}$$

The evolved joint state is

$$\begin{aligned} \rho_{SE}(t) &= U(t)(\rho_S \otimes \rho_E)U^\dagger(t) \\ &= (c\mathbb{I} - idS)(\rho_S \otimes \rho_E)(c\mathbb{I} + idS) \\ &= c^2(\rho_S \otimes \rho_E) + d^2S(\rho_S \otimes \rho_E)S - icd[S, \rho_S \otimes \rho_E]. \end{aligned} \tag{42}$$

Using the SWAP identity,

$$S(\rho_S \otimes \rho_E)S = \rho_E \otimes \rho_S. \tag{43}$$

Taking the partial trace over the environment gives

$$\rho_S(t) = c^2\rho_S + d^2\rho_E - icd\ \text{Tr}_E([S, \rho_S \otimes \rho_E]). \tag{44}$$

We now evaluate the commutator term. Since

$$S = \frac{1}{2}\left(\mathbb{I} + \sum_j \sigma_j \otimes \sigma_j\right), \tag{45}$$

only the Pauli part contributes to the commutator. Hence

$$\begin{aligned}\mathrm{Tr}_E([S, \rho_S \otimes \rho_E]) &= \frac{1}{2}\sum_j \mathrm{Tr}_E\big([\sigma_j \otimes \sigma_j, \rho_S \otimes \rho_E]\big) \\ &= \frac{1}{2}\sum_j \mathrm{Tr}_E\big(\sigma_j\rho_S \otimes \sigma_j\rho_E - \rho_S\sigma_j \otimes \rho_E\sigma_j\big).\end{aligned} \tag{46}$$

Using

$$\mathrm{Tr}(\sigma_j\rho_E) = \mathrm{Tr}(\rho_E\sigma_j) = e_j, \tag{47}$$

we get

$$\begin{aligned}\mathrm{Tr}_E([S, \rho_S \otimes \rho_E]) &= \frac{1}{2}\sum_j e_j(\sigma_j\rho_S - \rho_S\sigma_j) \\ &= \frac{1}{2}\sum_j e_j[\sigma_j, \rho_S].\end{aligned} \tag{48}$$

Now substitute

$$\rho_S = \frac{1}{2}\left(\mathbb{I} + \sum_k s_k\sigma_k\right). \tag{49}$$

Then

$$\begin{aligned}[\sigma_j, \rho_S] &= \frac{1}{2}\sum_k s_k[\sigma_j, \sigma_k] \\ &= \frac{1}{2}\sum_k s_k\left(2i\sum_\ell \varepsilon_{jk\ell}\sigma_\ell\right) \\ &= i\sum_{k,\ell} s_k\varepsilon_{jk\ell}\sigma_\ell.\end{aligned} \tag{50}$$

Therefore

$$\begin{aligned}\mathrm{Tr}_E([S, \rho_S \otimes \rho_E]) &= \frac{i}{2}\sum_{j,k,\ell} e_j s_k \varepsilon_{jk\ell}\sigma_\ell \\ &= -\frac{i}{2}(\vec{s} \times \vec{e}) \cdot \vec{\sigma}.\end{aligned} \tag{51}$$

Substituting this result into Equation (44), we obtain

$$\begin{aligned}\rho_S(t) &= c^2\rho_S + d^2\rho_E - icd\left[-\frac{i}{2}(\vec{s} \times \vec{e}) \cdot \vec{\sigma}\right] \\ &= c^2\rho_S + d^2\rho_E - \frac{cd}{2}(\vec{s} \times \vec{e}) \cdot \vec{\sigma}.\end{aligned} \tag{52}$$

Finally, using

$$\rho_S = \frac{1}{2}(\mathbb{I} + \vec{s} \cdot \vec{\sigma}), \qquad \rho_E = \frac{1}{2}(\mathbb{I} + \vec{e} \cdot \vec{\sigma}), \tag{53}$$

we find

$$\rho_S(t) = \frac{1}{2}\left[\mathbb{I} + \left(c^2\vec{s} + d^2\vec{e} - cd(\vec{s} \times \vec{e})\right) \cdot \vec{\sigma}\right]. \tag{54}$$

Therefore

$$\vec{s}(t) = c^2\vec{s} + d^2\vec{e} - cd(\vec{s} \times \vec{e}). \tag{55}$$

This completes the proof. □

Taking the z-component of Equation (30) gives

$$z(t) = c^2 s_z + d^2 e_z - cd\big(s_x e_y - s_y e_x\big), \tag{56}$$

where $\vec{s} = (s_x, s_y, s_z)$ and $\vec{e} = (e_x, e_y, e_z)$.

Lemma 1. *Let $\vec{a} \in \mathbb{R}^3$ and $b \in \mathbb{R}$, and consider*

$$f(\vec{e}) = \vec{a} \cdot \vec{e} + b, \qquad |\vec{e}| \leq 1. \tag{57}$$

Then the extrema of f over the Bloch ball occur on $|\vec{e}| = 1$ and are

$$f_{\max\,/\,\min} = b \pm |\vec{a}|. \tag{58}$$

Proof. For any $\vec{e}$ with $|\vec{e}| \leq 1$,

$$f(\vec{e}) - b = \vec{a} \cdot \vec{e} \leq |\vec{a}|\,|\vec{e}| \leq |\vec{a}|, \tag{59}$$

so $f(\vec{e}) \leq b + |\vec{a}|$. The upper bound is achieved for $\vec{e} = \vec{a}/|\vec{a}|$ when $\vec{a} \neq 0$. A symmetric argument with $\vec{e} = -\vec{a}/|\vec{a}|$ gives the lower bound $b - |\vec{a}|$. □

Remark 1. *Because $f(\vec{e})$ is affine in $\vec{e}$, its extrema over the Bloch ball occur on the boundary $|\vec{e}| = 1$. Thus pure environment states determine the extremal values, while mixed states yield intermediate values inside the interval.*

Corollary 1. *For fixed $\vec{s}$ and t, all factorized initial states $\rho_{SE}(0) = \rho_S \otimes \rho_E$ evolving under H_{ex} satisfy*

$$z_{\min}(t) \leq z(t) \leq z_{\max}(t), \tag{60}$$

where

$$z_{\max\,/\,\min}(t) = c^2 s_z \pm |d| \sqrt{d^2 + c^2\big(s_x^2 + s_y^2\big)}. \tag{61}$$

The absolute value of $d = \sin(2Jt)$ ensures that the interval remains correctly ordered, $z_{\min}(t) \leq z_{\max}(t)$, for all evolution times, including intervals in which $d < 0$.

Proof. From Equation (56) we write

$$z(t) = b(t) + \vec{a}(t) \cdot \vec{e}, \tag{62}$$

with

$$b(t) = c^2 s_z, \qquad \vec{a}(t) = \big(cd\, s_y,\ -cd\, s_x,\ d^2\big). \tag{63}$$

The norm is

$$\begin{aligned} |\vec{a}(t)|^2 &= c^2 d^2 \big(s_x^2 + s_y^2\big) + d^4 \\ &= d^2 \Big[d^2 + c^2 \big(s_x^2 + s_y^2\big)\Big]. \end{aligned} \tag{64}$$

Therefore,

$$|\vec{a}(t)| = |d| \sqrt{d^2 + c^2\big(s_x^2 + s_y^2\big)}. \tag{65}$$

Applying Lemma 1 with $b = b(t)$ and $\vec{a} = \vec{a}(t)$ gives

$$\begin{aligned} z_{\max\,/\,\min}(t) &= b(t) \pm |\vec{a}(t)| \\ &= c^2 s_z \pm |d| \sqrt{d^2 + c^2\left(s_x^2 + s_y^2\right)}. \end{aligned} \tag{66}$$

□

Geometric Interpretation of the Exchange Dynamics

Equation (30) admits a simple geometric interpretation, illustrated in Figure 2. For factorized initial states, the reduced Bloch vector is given by

$$\vec{s}(t) = c^2\vec{s} + d^2\vec{e} - cd(\vec{s} \times \vec{e}), \tag{67}$$

where the vectors $\vec{s}$, $\vec{e}$, and $\vec{s} \times \vec{e}$ are linearly independent whenever $\vec{s}$ and $\vec{e}$ are not parallel.

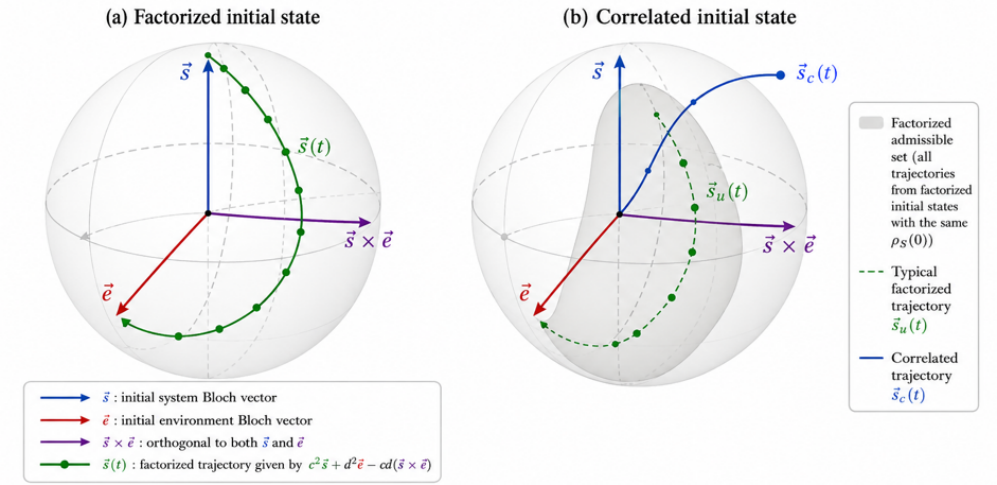


Figure 2. Geometric interpretation of the reduced dynamics under the isotropic Heisenberg exchange interaction. (**a**) For factorized initial states, the reduced Bloch vector evolves according to Equation (30), $\vec{s}(t) = c^2\vec{s} + d^2\vec{e} - cd(\vec{s} \times \vec{e})$, where $\vec{s}$ and $\vec{e}$ denote the initial system and environment Bloch vectors, respectively. The resulting trajectory (green) is generally three-dimensional because of the exchange term $\vec{s} \times \vec{e}$. (**b**) Schematic illustration of the effect of initial system–environment correlations. The dashed green curve represents a typical factorized trajectory, while the shaded gray region schematically represents the family of trajectories compatible with factorized initial states sharing the same calibrated reduced system state. The solid blue curve illustrates a representative correlated trajectory that leaves this family and may violate the factorized envelope, thereby certifying initial system–environment correlations.

Figure 2a illustrates this evolution. The blue and red arrows denote the initial system and environment Bloch vectors, respectively, while the purple arrow represents the vector $\vec{s} \times \vec{e}$, which is orthogonal to both. The reduced Bloch vector (green curve) evolves from the initial system vector towards the environment vector while simultaneously acquiring an orthogonal component generated by the exchange interaction. Consequently, the trajectory is generally not confined to the plane spanned by $\vec{s}$ and $\vec{e}$. Instead, it evolves within the three-dimensional subspace generated by $\{\vec{s}, \vec{e}, \vec{s} \times \vec{e}\}$. Only when $\vec{s} \times \vec{e} = \mathbf{0}$, that is, when the two Bloch vectors are parallel or antiparallel, does the trajectory remain planar.

The same dynamics follow naturally from the exchange unitary

$$U(t) = \cos(2Jt)\,\mathbb{I} - i\sin(2Jt)\,S,$$

where S is the SWAP operator (up to an overall global phase). The coefficients $c = \cos(2Jt)$ and $d = \sin(2Jt)$ continuously interpolate between the identity operation and a complete

SWAP, causing the reduced Bloch vector to evolve smoothly between the system and environment Bloch vectors while generating the orthogonal exchange contribution.

Figure 2b illustrates the effect of initial system–environment correlations. The dashed green curve represents a typical trajectory generated by a factorized initial state, whereas the solid blue curve represents a correlated trajectory. Initial correlations contribute through the correlation tensor and modify the reduced dynamics beyond Equation (30), producing trajectories that cannot, in general, be generated by any factorized preparation having the same calibrated reduced state. These deviations may lead to violations of the factorized envelope derived in Corollary 1, providing the operational basis for the single-observable witness introduced in this work (Appendix A).

5. Witness of Initial Correlations

We can now state the witness formally.

Theorem 1 (Minimal-observable witness)**.** *Let the system evolve under H_{ex} with known initial $\rho_S(0) = \frac{1}{2}(\mathbb{I} + \vec{s}\cdot\vec{\sigma})$. For each t, let $[z_{\min}(t), z_{\max}(t)]$ be the factorized envelope of Corollary 1. If for some t^* the experimentally observed value $\tilde{z}(t^*)$ satisfies*

$$\tilde{z}(t^*) \notin [z_{\min}(t^*), z_{\max}(t^*)], \tag{68}$$

then the initial joint state $\rho_{SE}(0)$ was not factorized. In particular, initial S-E correlations are certified.

Proof. Corollary 1 shows that every factorized state $\rho_{SE}(0) = \rho_S \otimes \rho_E$ with the given ρ_S produces $z(t)$ in the interval $[z_{\min}(t), z_{\max}(t)]$. Thus

$$\mathcal{R}(t) = \left\{ z(t) \mid \rho_{SE}(0) = \rho_S \otimes \rho_E \right\} = [z_{\min}(t), z_{\max}(t)]. \tag{69}$$

If $\tilde{z}(t^*)$ lies outside this interval, there is no product state consistent with the observation at t^*, so $\rho_{SE}(0)$ cannot be factorized. □

6. Examples: Three Canonical Initial States

In the protocol as implemented in the laboratory, only the reduced system state $\rho_S(0)$ is calibrated experimentally; the joint state $\rho_{SE}(0)$ is unknown and may or may not be correlated. In the following examples, by contrast, we *theoretically specify* a particular joint initial state $\rho_{SE}(0)$ in order to analyze the performance of the witness. The corresponding calibrated system state is always obtained as $\rho_S(0) = \mathrm{Tr}_E[\rho_{SE}(0)]$, matching what an experimentalist would have determined in the initial calibration step. The subsequent comparison between the correlated trajectory $z^{(\mathrm{corr})}(t)$ and the factorized envelope $\mathcal{R}(t)$ is therefore carried out using only system data and the known Hamiltonian, exactly as in the operational protocol.

We now illustrate the witness using the three families of initial states analyzed in Ref. [23]. In each case we:

1. Specify the (possibly correlated) initial state $\rho_{SE}(0)$;
2. Determine the calibrated reduced state $\rho_S(0)$ and its Bloch vector $\vec{s}(0)$;
3. Compute the correlated trajectory $z^{(\mathrm{corr})}(t)$; and
4. Compare $z^{(\mathrm{corr})}(t)$ with the factorized envelope $[z_{\min}(t), z_{\max}(t)]$.

Whenever $z^{(\mathrm{corr})}(t)$ leaves the envelope, the witness detects initial correlations using only the single observable $z(t)$.

For convenience we use the dimensionless variable Jt so that

$$c = \cos(2Jt), \qquad d = \sin(2Jt).$$

6.1. Example 1: Maximally Entangled Bell-like State

We first consider a maximally entangled initial state of S and E,

$$\rho_{SE}(0) = |\Psi\rangle\langle\Psi|, \qquad |\Psi\rangle = \tfrac{1}{\sqrt{2}}\big(|01\rangle + i\,|10\rangle\big). \tag{70}$$

Tracing out the environment gives a maximally mixed reduced state

$$\rho_S(0) = \mathrm{Tr}_E[\rho_{SE}(0)] = \tfrac{1}{2}\,\mathbb{I}, \qquad \vec{s}(0) = \vec{0}, \qquad z(0) = 0. \tag{71}$$

Thus, based solely on system information at $t = 0$, this preparation is indistinguishable from an uncorrelated product state with the same $\rho_S(0)$.

Reduced system trajectory. We use the convention

$$\sigma_z\,|0\rangle = |0\rangle, \qquad \sigma_z\,|1\rangle = -\,|1\rangle. \tag{72}$$

For the initial Bell-like state

$$|\Psi\rangle = \frac{1}{\sqrt{2}}(|01\rangle + i\,|10\rangle) \tag{73}$$

and the partial-SWAP unitary

$$U(t) = c\,\mathbb{I} - id\,S, \qquad c = \cos(2Jt), \qquad d = \sin(2Jt), \tag{74}$$

the evolved joint state is

$$\begin{aligned} |\Psi(t)\rangle &= U(t)\,|\Psi\rangle \\ &= \frac{1}{\sqrt{2}}[(c+d)\,|01\rangle + i(c-d)\,|10\rangle]. \end{aligned} \tag{75}$$

Tracing out the environment therefore gives

$$\rho_S(t) = \begin{pmatrix} p_0(t) & 0 \\ 0 & 1-p_0(t) \end{pmatrix}, \qquad p_0(t) = \frac{1}{2}[1+\sin(4Jt)]. \tag{76}$$

Hence the correlated single-axis observable is

$$\begin{aligned} z^{(\mathrm{corr})}(t) &= \left\langle \sigma_z^S \right\rangle(t) \\ &= p_0(t) - [1-p_0(t)] \\ &= \sin(4Jt). \end{aligned} \tag{77}$$

Factorized comparison envelope. To apply the witness, we compare $z^{(\mathrm{corr})}(t)$ with the set of all *factorized* preparations that are consistent with the same calibrated $\rho_S(0) = \mathbb{I}/2$. For any such state, the initial system Bloch vector satisfies $\vec{s}(0) = \vec{0}$, so Equation (56) reduces to

$$z(t) = d^2\,e_z, \qquad d = \sin(2Jt), \qquad e_z \in [-1,1]. \tag{78}$$

Optimizing over e_z yields the factorized envelope

$$z_{\min\,/\,\max}(t) = \pm\sin^2(2Jt), \tag{79}$$

and therefore every product initial state must satisfy

$$-\sin^2(2Jt) \le z(t) \le \sin^2(2Jt).$$

Witness violation and figure interpretation. Figure 3 compares the correlated trajectory $z^{(\mathrm{corr})}(t) = \sin(4Jt)$ (black curve) with the factorized envelope $[z_{\min}(t), z_{\max}(t)]$ (blue shaded region). At the witness time

$$t^* = \frac{\pi}{8J}, \tag{80}$$

we have

$$\sin(4Jt^*) = 1, \qquad \sin^2(2Jt^*) = \frac{1}{2}. \tag{81}$$

Therefore,

$$z^{(\mathrm{corr})}(t^*) = 1, \tag{82}$$

whereas every factorized initial state compatible with the same calibrated reduced state satisfies

$$z(t^*) \in \left[-\frac{1}{2}, \frac{1}{2}\right]. \tag{83}$$

The red marker in Figure 3 therefore lies above the upper factorized bound. Since no product initial state with the same calibrated $\rho_S(0)$ can reproduce this value, the observation certifies initial system–environment correlations using only the single observable $z(t)$.

Experimental note. In practice, $z(t) = \langle \sigma_z^S \rangle(t)$ is obtained by repeatedly preparing the system and performing a projective measurement of σ_z^S at time t, then averaging the binary outcomes. This procedure uses only a single measurement axis and is standard in NMR, trapped ions, superconducting qubits, and NV centers.

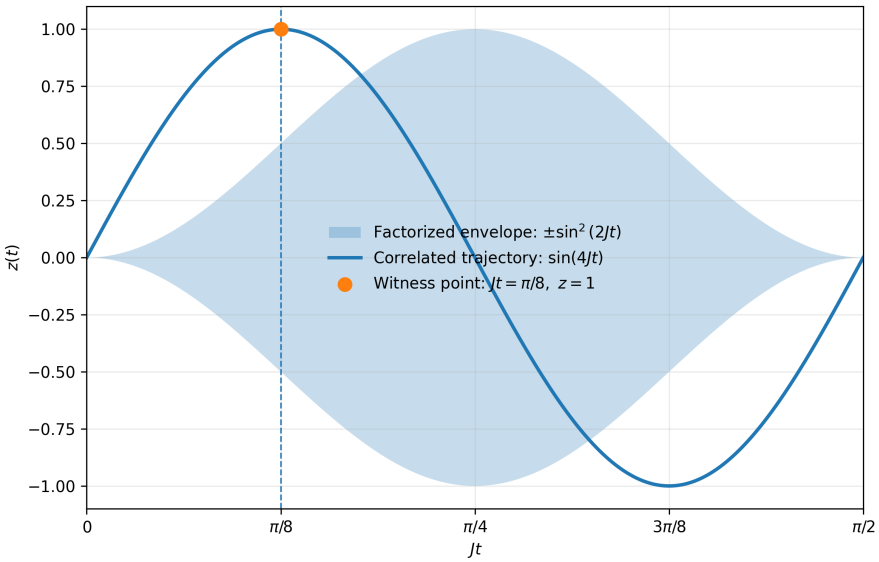


Figure 3. Example 1. The black curve shows the corrected correlated trajectory $z^{(\mathrm{corr})}(t) = \sin(4Jt)$ for the maximally entangled initial state. The blue shaded region is the factorized envelope $z_{\min\,/\,\max}(t) = \pm\sin^2(2Jt)$ for all product states with $\rho_S(0) = \mathbb{I}/2$. At $t^* = \pi/(8J)$, indicated by the red marker, the correlated value is $z^{(\mathrm{corr})}(t^*) = 1$, whereas the factorized interval is $[-1/2, 1/2]$. The trajectory therefore lies above the upper factorized bound, certifying initial correlations using only $z(t)$.

6.2. Example 2: Mixture of a Product State and an Entangled State

We next consider a family of mixed initial states interpolating between a product state and the maximally entangled state of Example 1:

$$\rho_{SE}(0) = p\,|01\rangle\langle 01| + (1-p)\,|\Psi\rangle\langle\Psi|, \qquad 0 \le p \le 1, \tag{84}$$

with $|\Psi\rangle$ as defined above. Tracing out the environment gives

$$\rho_S(0) = \begin{pmatrix} \frac{1+p}{2} & 0 \\ 0 & \frac{1-p}{2} \end{pmatrix}, \qquad \vec{s}(0) = (0,0,p), \qquad z(0) = p, \tag{85}$$

so the calibrated system state contains a finite polarization p along z.

Correlated trajectory. Using the singlet-triplet decomposition as before, evolving under $H_{\mathrm{ex}} = J\,\vec{\sigma}_S \cdot \vec{\sigma}_E$ and tracing out E yields the correlated single-axis observable

$$z^{(\mathrm{corr})}(t) = p\cos(4Jt) + (1-p)\sin(4Jt). \tag{86}$$

which continuously connects to Example 1 when $p = 0$.

Factorized comparison envelope. To construct the witness, we compare $z^{(\mathrm{corr})}(t)$ with all *factorized* initial states consistent with the same calibrated $\rho_S(0)$. For any such product state, $\vec{s}(0) = (0,0,p)$, so Equation (56) reduces to

$$z(t) = c^2 p + d^2 e_z, \qquad e_z \in [-1,1], \tag{87}$$

with $c = \cos(2Jt)$ and $d = \sin(2Jt)$. Optimizing over e_z yields the envelope

$$z_{\min\,/\,\max}(t) = \cos^2(2Jt)\,p \pm \sin^2(2Jt), \tag{88}$$

and therefore every factorized initial state with the same $\rho_S(0)$ must satisfy

$$\cos^2(2Jt)\,p - \sin^2(2Jt) \;\le\; z(t) \;\le\; \cos^2(2Jt)\,p + \sin^2(2Jt).$$

Witness violation. A convenient witness time is

$$t^* = \frac{\pi}{8J},$$

for which

$$z^{(\mathrm{corr})}(t^*) = 1-p, \qquad z_{\min\,/\,\max}(t^*) = \left[\frac{p-1}{2}, \frac{p+1}{2}\right].$$

Violation occurs whenever

$$1 - p > \frac{p+1}{2},$$

which is equivalent to

$$p < \frac{1}{3}.$$

Thus, for

$$0 \le p < \frac{1}{3},$$

the correlated trajectory lies above the upper factorized bound at t^*, thereby certifying initial system–environment correlations using only the single observable $z(t)$. For larger values of p, no violation occurs at this particular witness time, although it may occur at other times.

Figure interpretation. Figure 4 shows the correlated trajectories $z^{(\mathrm{corr})}(t)$ (black curves) together with the corresponding factorized envelopes (blue shaded regions) for three representative values of p. The panels illustrate how decreasing p increases the weight of the entangled component and eventually produces a clear envelope crossing. For $p = 0.6$ the correlated curve remains inside the envelope at t^*; for $p = 0.2$ and $p = 0.1$ the correlated value at the red marker lies strictly outside the envelope, certifying initial correlations with a single observable.

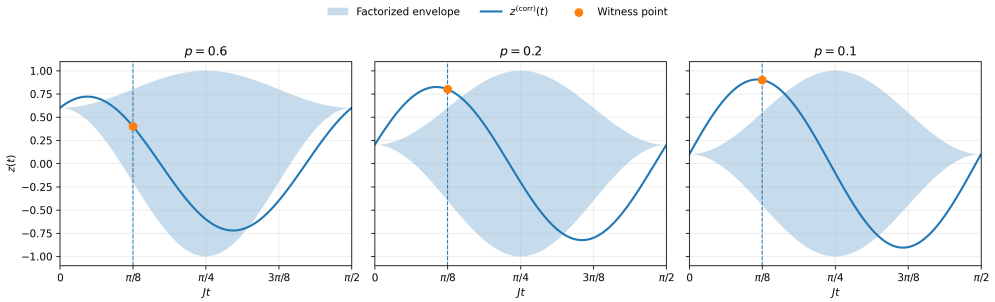


Figure 4. Example 2. The blue shaded region shows the factorized envelope $z_{\min\,/\,\max}(t) = p\cos^2(2Jt) \pm \sin^2(2Jt)$ for all product initial states compatible with the calibrated reduced state $\rho_S(0)$. The black curves show the corrected correlated trajectories $z^{(\mathrm{corr})}(t) = p\cos(4Jt) + (1-p)\sin(4Jt)$ for different values of the mixing parameter p. At the witness time $t^* = \pi/(8J)$ (red marker), the correlated value is $z^{(\mathrm{corr})}(t^*) = 1 - p$, while the corresponding factorized upper bound is $z_{\max}(t^*) = (1+p)/2$. For $p < 1/3$, the correlated trajectory exceeds the upper factorized bound, thereby certifying initial system–environment correlations using only the single observable $z(t)$.

6.3. Example 3: Mixture with the Maximally Mixed State

Finally, we consider a different type of mixture in which the entangled state of Example 1 is diluted by the maximally mixed two-qubit state:

$$\rho_{SE}(0) = p\,\frac{\mathbb{I}_4}{4} + (1-p)\,|\Psi\rangle\langle\Psi|\,, \qquad 0 \le p \le 1, \tag{89}$$

where $|\Psi\rangle$ is the maximally entangled state used previously. Tracing out the environment yields

$$\rho_S(0) = p\,\frac{\mathbb{I}_2}{2} + (1-p)\frac{\mathbb{I}_2}{2} = \frac{\mathbb{I}_2}{2}, \tag{90}$$

so the calibrated system state is maximally mixed, with $\vec{s}(0) = \vec{0}$ and $z(0) = 0$, regardless of p.

Correlated trajectory. The maximally mixed part is invariant under all unitary dynamics and therefore does not contribute to $z(t)$. Only the entangled component evolves nontrivially, and using the result of Example 1 we obtain

$$z^{(\mathrm{corr})}(t) = (1-p)\sin(4Jt). \tag{91}$$

which continuously interpolates between the fully entangled trajectory ($p = 0$) and a flat signal ($p = 1$).

Factorized comparison envelope. Since $\rho_S(0) = \mathbb{I}_2/2$ for all p, the factorized initial states have $\vec{s}(0) = \vec{0}$ and the envelope reduces to the same form as in Example 1:

$$z_{\min\,/\,\max}(t) = \pm\sin^2(2Jt). \tag{92}$$

Therefore, every factorized initial state compatible with the same calibration must satisfy

$$-\sin^2(2Jt) \;\le\; z(t) \;\le\; \sin^2(2Jt).$$

Witness violation and figure interpretation. A violation occurs whenever

$$\left|z^{(\mathrm{corr})}(t)\right| = (1-p)\,|\sin(4Jt)| > \sin^2(2Jt). \tag{93}$$

Using

$$|\sin(4Jt)| = 2\,|\sin(2Jt)\cos(2Jt)|, \tag{94}$$

and assuming $\sin(2Jt) \neq 0$, the violation condition can be written as

$$2(1-p)|\cos(2Jt)| > |\sin(2Jt)|, \tag{95}$$

or equivalently,

$$|\tan(2Jt)| < 2(1-p). \tag{96}$$

For every $p < 1$, the right-hand side of Equation (96) is strictly positive. Therefore, the condition is satisfied for sufficiently small but nonzero values of t.

Equivalently, near $t = 0$,

$$z^{(\mathrm{corr})}(t) = (1-p)\sin(4Jt) = 4J(1-p)t + \mathcal{O}(t^3), \tag{97}$$

whereas the factorized envelope behaves as

$$\sin^2(2Jt) = 4J^2t^2 + \mathcal{O}(t^4). \tag{98}$$

Thus, for every $p < 1$, the correlated signal grows linearly in t near the origin, while the width of the factorized envelope grows quadratically. Consequently, there always exists a sufficiently small nonzero time at which the correlated trajectory lies outside the factorized envelope. Although the reduced state is maximally mixed and contains no evidence of correlations at $t = 0$, later measurements of the single observable $z(t)$ can therefore reveal the hidden initial system–environment correlations for every $p < 1$. Figure 5 illustrates this behavior. The blue shaded regions indicate the factorized envelope, while the black curves show $z^{(\mathrm{corr})}(t)$ for three representative values of p. For every $p < 1$, the correlated trajectory leaves the factorized envelope at sufficiently small but nonzero times because the correlated signal grows linearly near $t = 0$, whereas the factorized envelope grows quadratically. However, at the particular witness time $t^* = \pi/(8J)$ indicated by the red marker, a violation occurs only when $p < 1/2$. Consequently, the panels with $p = 0.4$ and $p = 0.1$ show a violation at the marked witness time, while the $p = 0.8$ trajectory can still leave the envelope at earlier, sufficiently small nonzero times. As $p \to 1$, the correlated signal vanishes and the initial state approaches the maximally mixed product state, consistently eliminating the witness violation.

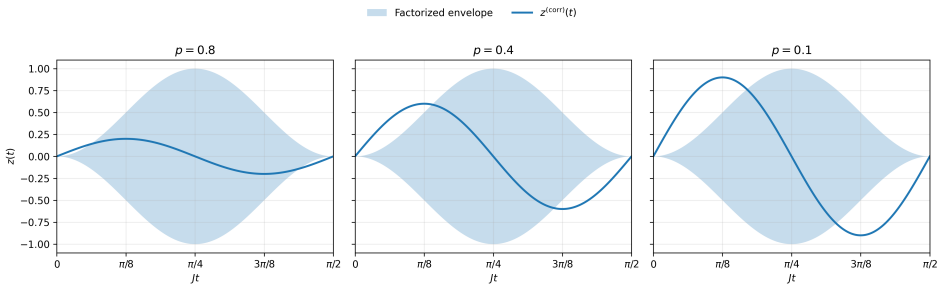


Figure 5. Example 3.The blue shaded region shows the factorized envelope $z_{\min\,/\,\max}(t) = \pm\sin^2(2Jt)$ for all product initial states compatible with the calibrated reduced state $\rho_S(0) = \mathbb{I}/2$. The black curves show the corrected correlated trajectories $z^{(\mathrm{corr})}(t) = (1-p)\sin(4Jt)$ for different values of the mixing parameter p. At the witness time $t^* = \pi/(8J)$, the correlated value is $z^{(\mathrm{corr})}(t^*) = 1-p$, while every factorized initial state satisfies $z(t^*) \in [-1/2, 1/2]$. For the chosen witness time $t^* = \pi/(8J)$, the correlated trajectory exceeds the upper factorized bound whenever $p < 1/2$, thereby certifying initial system–environment correlations using only the single observable $z(t)$.

7. Extension to an Exactly Solvable Infinite-Bath Model

While the isotropic Heisenberg exchange provides a minimal and fully controllable setting for developing the single-observable witness, it is natural to ask whether the

same logic survives in more conventional open-system models with infinite environments. In this section, we demonstrate that the witness extends naturally to the exactly solvable pure-dephasing spin–boson model, which is a standard benchmark in the theory of open quantum systems.

7.1. Pure-Dephasing Spin–Boson Hamiltonian

We consider the Hamiltonian [Equation (4.28) of Ref. [1]]

$$H = \frac{\omega_0}{2}\sigma_z + \sum_k \omega_k b_k^\dagger b_k + \sigma_z \sum_k \left(g_k b_k^\dagger + g_k^* b_k \right), \tag{99}$$

where σ_z acts on the system qubit and $\{b_k, b_k^\dagger\}$ are bosonic operators describing an infinite environment. This model generates pure dephasing: the system populations remain constant, while the coherences decay in time. Importantly, the reduced dynamics admit a closed-form solution for factorized initial states, making this model analytically tractable.

7.2. Reduced Dynamics for Factorized Initial States

Assuming an initially factorized state $\rho_{SE}(0) = \rho_S(0) \otimes \rho_E(0)$, the reduced system state at time t is given by

$$\rho_S(t) = \begin{pmatrix} \rho_{00}(0) & \rho_{01}(0)\, e^{-\Gamma(t)} \\ \rho_{10}(0)\, e^{-\Gamma(t)} & \rho_{11}(0) \end{pmatrix}, \tag{100}$$

where $\Gamma(t) \geq 0$ is the decoherence function corresponding to the assumed bath model (for example, a thermal bath with known spectral density and temperature). Throughout this section, the null hypothesis is that the initial state is factorized,

$$\rho_{SE}(0) = \rho_S(0) \otimes \rho_E(0),$$

the reduced system state $\rho_S(0)$ is fixed by the initial calibration, and the bath is completely characterized through the known decoherence function $\Gamma(t)$. Its explicit form is not required for our purposes; we use only that $\Gamma(0) = 0$ and $e^{-\Gamma(t)} \in [0, 1]$ for all t.

Since $\langle \sigma_z \rangle(t)$ is constant under pure dephasing, we focus on a single transverse observable,

$$x(t) = \langle \sigma_x \rangle(t) = \mathrm{Tr}_S[\rho_S(t)\sigma_x]. \tag{101}$$

From Equation (100), one obtains

$$x(t) = x(0)\, e^{-\Gamma(t)}, \tag{102}$$

where $x(0) = \langle \sigma_x \rangle(0)$ is fixed by the initial calibration of the reduced system state. Consequently, under the factorized null hypothesis, the complete admissible prediction is determined jointly by the calibrated initial coherence $x(0)$ and the known decoherence function $\Gamma(t)$.

7.3. Factorized Envelope and Witness

For every factorized initial state compatible with the calibrated reduced system state,

$$|x(t)| \leq |x(0)|\, e^{-\Gamma(t)}. \tag{103}$$

This inequality defines the admissible factorized prediction for the calibrated initial coherence. Therefore, any experimentally observed value satisfying

$$|x(t)| > |x(0)| e^{-\Gamma(t)}$$

cannot arise from any factorized initial state sharing the same calibrated reduced system state and therefore certifies initial system–environment correlations.

This inequality defines a time-dependent *factorized envelope* for the single observable $x(t)$ under the pure-dephasing dynamics. It represents the entire set of values compatible with the standard product assignment $\rho_{SE}(0) = \rho_S(0) \otimes \rho_E(0)$ for an infinite bosonic bath.

Unlike the exchange model, the pure-dephasing dynamics admit no further optimization over environmental degrees of freedom beyond the decoherence function $\Gamma(t)$. Consequently, the factorized envelope takes a particularly simple form, while any deviation from it directly reflects the presence of initial system–environment correlations.

If, for some time t^*, an experimentally observed value satisfies

$$|\tilde{x}(t^*)| > |x(0)|e^{-\Gamma(t^*)}, \tag{104}$$

then no factorized initial state sharing the same calibrated reduced system state and evolving under the assumed bath model can reproduce the observation. Such a violation therefore certifies initial system–environment correlations.

This example demonstrates that the single-observable witness is not restricted to finite environments or exchange-type interactions. Even in a paradigmatic infinite-bath model with analytically solvable reduced dynamics, factorized initial states generate a sharply constrained admissible region for a single system observable. Initial correlations modify the coherence dynamics and can drive the signal outside this region, providing a clear and experimentally accessible signature of correlated preparations.

8. Performance Analysis of the Minimal-Observable Witness

The factorized-envelope witness developed in the previous sections provides a simple criterion for certifying initial system–environment correlations using measurements of only a single calibrated observable. In this section we discuss its operational performance, practical requirements, and inherent limitations. Rather than introducing a new detection criterion, our goal is to clarify how the witness should be interpreted in realistic experimental settings and to identify the situations in which it provides its greatest advantage.

8.1. One-Sided Nature of the Witness

The factorized-envelope construction is intentionally designed as a *one-sided witness*. For every calibrated reduced state $\rho_S(0)$ and known interaction Hamiltonian, the interval $\mathcal{R}(t) = [z_{\min}(t), z_{\max}(t)]$ contains all trajectories that can arise from factorized initial states. Consequently,

$$z(t) \notin \mathcal{R}(t) \quad \Longrightarrow \quad \rho_{SE}(0) \neq \rho_S(0) \otimes \rho_E(0), \tag{105}$$

providing an unambiguous certification of initial system–environment correlations.

The converse, however, does not generally hold. A correlated initial state may still generate a trajectory lying entirely inside the factorized envelope, because the correlation contribution to the reduced dynamics can be indistinguishable from that produced by an appropriate factorized environment state. Remaining inside the envelope therefore cannot be interpreted as evidence that the initial state was uncorrelated.

This behavior is characteristic of witness-based methods throughout quantum information theory. For example, entanglement witnesses certify entanglement whenever their inequality is violated, while many entangled states remain undetected. Similarly, Bell inequalities provide sufficient but not necessary conditions for nonlocality. The present protocol should therefore be interpreted in exactly the same spirit: violation certifies initial correlations, whereas absence of violation simply leaves the possibility of hidden correlations open.

The advantage of this approach is that every detected event is rigorous. Whenever the observed trajectory exits the factorized envelope, the existence of initial correlations follows directly from the incompatibility between the measured dynamics and every admissible factorized preparation. No optimization, reconstruction of the reduced state, or access to the environment is required.

8.2. Experimental Resource Requirements

The principal motivation for the present protocol is the reduction in experimental overhead. Most existing system-only detection methods require repeated state preparation together with reconstruction of the reduced density matrix at multiple evolution times. Such procedures generally involve measurements of several noncommuting observables and the subsequent implementation of state tomography.

By contrast, the present protocol requires only a one-time calibration of the initial reduced state $\rho_S(0)$. Once this calibration has been completed, all subsequent measurements are performed along a single fixed axis, namely

$$z(t) = \langle \sigma_z^S \rangle(t). \tag{106}$$

No reconstruction of $\rho_S(t)$ is performed during the evolution, and no measurements on the environment are required.

The simplification comes at the cost of assuming that the interaction Hamiltonian is known. Knowledge of the joint dynamics makes it possible to compute the factorized envelope analytically, which then serves as the reference model against which experimental observations are compared. Consequently, the protocol is particularly attractive in physical platforms where the interaction Hamiltonian has already been accurately characterized, including NMR systems, trapped ions, superconducting circuits, and other highly controlled quantum devices.

The present witness therefore complements rather than replaces existing system-only detection methods. Protocols based on trace-distance growth or full state tomography require fewer assumptions regarding the interaction model but demand substantially greater measurement resources. Conversely, our protocol exchanges detailed Hamiltonian knowledge for a significant reduction in experimental complexity.

Table 1 highlights the complementary nature of the present protocol. Unlike tomography-based approaches, our method does not require repeated reconstruction of the reduced density operator during the evolution. Instead, after a one-time calibration of the initial reduced state, all subsequent measurements are performed on a single fixed observable. This simplification is achieved by assuming that the system–environment Hamiltonian is known, allowing the factorized compatibility envelope to be computed in advance. The proposed witness should therefore be viewed as complementary to existing methods rather than as a universal replacement. It is particularly advantageous in well-characterized quantum platforms, where accurate Hamiltonian models are available and reducing experimental measurement overhead is a primary objective.

Table 1. Comparison of representative approaches for detecting initial system–environment correlations.

Method	Ham.	Tomo.	Repeat
Trace distance	No	Yes	Yes
Tomography	No	Yes	Yes
This work	Yes	No [a]	No

[a] After one-time calibration of $\rho_S(0)$.

8.3. Sensitivity to Measurement Uncertainty

In practice, every measured expectation value is affected by finite sampling statistics and experimental imperfections. Suppose that the experimentally observed signal is

$$z_{\mathrm{exp}}(t) = z(t) + \delta z(t), \tag{107}$$

where $\delta z(t)$ represents the combined contribution of statistical fluctuations and measurement noise.

The witness remains applicable provided the experimental uncertainty is properly incorporated into the comparison with the theoretical envelope. Instead of comparing the measured value directly with $\mathcal{R}(t)$, one compares the corresponding confidence interval

$$z_{\mathrm{exp}}(t) \pm \Delta z(t) \tag{108}$$

with the factorized region. Only when the confidence interval lies entirely outside $\mathcal{R}(t)$ can initial system–environment correlations be certified with the chosen confidence level.

The robustness of the witness therefore depends primarily on the separation between the observed trajectory and the factorized envelope. Large violations remain detectable even in the presence of moderate measurement uncertainty, whereas trajectories lying very close to the boundary require improved statistical precision. This behavior is common to most experimentally implemented witness protocols and does not affect the theoretical validity of the certification criterion.

8.4. Scope and Limitations

The present work establishes the compatibility-envelope construction for two exactly solvable open-system models. The isotropic Heisenberg exchange provides an analytically tractable finite-dimensional benchmark in which the factorized envelope can be derived in closed form. The exactly solvable spin–boson model considered in the following section demonstrates that the same single-observable logic extends naturally to an infinite-dimensional environment.

We emphasize, however, that these models are intended to establish the general methodology rather than to represent every physically relevant environment. In particular, the spin–boson example describes pure-dephasing dynamics, whereas more general dissipative environments involving energy exchange remain to be investigated.

Another important limitation follows directly from the one-sided nature of the proposed witness. Specifically, the criterion is sufficient, but not necessary, for detecting initial system–environment correlations. Whenever the observed trajectory exits the factorized compatibility envelope, the initial state cannot have been factorized, thereby providing a rigorous certification of initial correlations. Conversely, trajectories that remain within the factorized envelope do not imply that the initial state was factorized since correlated initial states may also generate dynamics consistent with the compatibility bounds. The present protocol should therefore be interpreted as a one-sided certification tool rather than a test for the absence of initial system–environment correlations. Developing stronger witnesses capable of reducing the number of correlated states that remain undetected while preserving the simplicity of single-observable measurements, constitutes an important direction for future work. A quantitative characterization of the detection efficiency of the present witness, namely the fraction of correlated initial states that produce observable violations of the factorized envelope, also lies beyond the scope of the present work.

Although every violation certifies initial system–environment correlations, correlated states whose trajectories remain inside the factorized envelope cannot be identified by the present protocol alone. Developing stronger witnesses capable of reducing the number of

correlated states that remain undetected by the witness, while preserving the simplicity of single-observable measurements, constitutes an interesting direction for future work. A quantitative characterization of the detection efficiency of the present witness, namely the fraction of correlated initial states that produce observable violations of the factorized envelope, lies beyond the scope of the present work. Such an analysis would require sampling correlated initial system–environment states according to an appropriate statistical measure and evaluating the corresponding detection probability. This represents an interesting direction for future research and would provide additional insight into the practical performance of the proposed single-observable witness. Despite these limitations, the proposed protocol demonstrates that initial system–environment correlations can be rigorously certified without state tomography, without repeated measurement of noncommuting observables, and without direct access to the environment. This substantial reduction in experimental resources makes the method an attractive complement to existing system-only approaches for detecting initial correlations in open quantum systems.

9. Conclusions

We have presented a single-observable protocol for certifying initial system–environment correlations in open quantum systems. For a qubit interacting with an environment through the isotropic Heisenberg exchange, we showed that a one-time calibration of the reduced system state, together with measurements of a single system observable, is sufficient to detect initial correlations without requiring state tomography, multiple state preparations, or direct access to the environment.

The central result is the derivation of an exact factorized envelope that bounds the dynamics of all product initial states compatible with the calibrated reduced system state. Any experimentally observed trajectory leaving this envelope excludes every factorized preparation sharing the same reduced state and therefore certifies the presence of initial system–environment correlations. A geometric interpretation of the reduced dynamics clarifies the origin of this constraint, while the examples demonstrate that the witness successfully detects correlations for several representative families of initial states.

The proposed protocol is inherently a one-sided certification method. Violation of the factorized envelope provides a rigorous and experimentally accessible witness of initial correlations, whereas remaining inside the envelope does not exclude their presence. The protocol therefore provides a sufficient, but not necessary, criterion for certifying correlated initial states.

Finally, we extended the same operational idea to the exactly solvable pure-dephasing spin–boson model with an infinite environment, where an analogous coherence envelope can be derived. This shows that the underlying principle is not restricted to finite-dimensional environments or exchange-type interactions but reflects a more general structural property of reduced dynamics generated from factorized initial states.

Our results demonstrate that surprisingly limited measurement resources can provide rigorous information about initial system–environment correlations. They also suggest a broader class of single-observable certification protocols for other interactions, higher-dimensional environments, and more general open quantum systems, bringing the experimental detection of initial correlations closer to practical implementation.

Author Contributions: Methodology, A.A.-N.; Validation, L.-A.W.; Formal analysis, R.R.C.; Investigation, A.A.-N.; Writing–original draft, A.A.-N.; Writing–review & editing, R.R.C.; Supervision, L.-A.W. All authors have read and agreed to the published version of the manuscript.

Funding: Ali Abu-Nada gets the financial support from the Sharjah Maritime Academy through the Project Seed Funding Scheme (Grant No. SMA-SF-001), entitled "Predicting System Evolution and Detecting Memory Effects in Quantum Dynamics using Reinforcement Learning."

L.-A.W. is supported by the Basque Country Government (Grant No. IT1470-22) and Grant No. PGC2018-101355-B-I00, funded by MCIN/AEI/10.13039/501100011033; the Ministry for Digital Transformation and Civil Service of the Spanish Government through the QUANTUM ENIA project call—Quantum Spain project; and the European Union through the Recovery, Transformation and Resilience Plan–NextGenerationEU, within the framework of the Digital Spain 2026 Agenda.

Data Availability Statement: The original contributions presented in this study are included in the article. Further inquiries can be directed to the corresponding author.

Conflicts of Interest: The authors declare no conflicts of interest.

Appendix A. Deviation from Partial Swap for Correlated Initial States

For factorized initial states $\rho_{SE}(0) = \rho_S \otimes \rho_E$, the reduced system Bloch vector obeys Equation (30),

$$\vec{s}(t) = c^2\vec{s} + d^2\vec{e} - cd\,(\vec{s} \times \vec{e}), \tag{A1}$$

which depends only on $(\vec{s}, \vec{e})$ and the Heisenberg parameters (c, d).

Equation (A1) therefore provides a complete description of the reduced dynamics whenever the initial state is factorized. In particular, all trajectories belonging to the factorized envelope derived in the main text are generated solely by varying the unknown environment Bloch vector $\vec{e}$ while keeping the calibrated system Bloch vector $\vec{s}$ fixed. To understand how initial system–environment correlations modify this picture, we now consider the most general two-qubit initial state.

For correlated initial states, it is convenient to use the full Bloch decomposition

$$\rho_{SE}(0) = \tfrac{1}{4}\Big(\mathbb{I}\otimes\mathbb{I} + \vec{s}\cdot\vec{\sigma}\otimes\mathbb{I} + \mathbb{I}\otimes\vec{e}\cdot\vec{\sigma} + \sum_{j,k} C_{jk}\,\sigma_j\otimes\sigma_k\Big), \tag{A2}$$

where $C_{jk} = \mathrm{Tr}[\rho_{SE}(0)\,\sigma_j\otimes\sigma_k]$ is the correlation tensor.

For product states one has

$$C_{jk} = s_j e_k, \tag{A3}$$

so we write

$$C_{jk} = s_j e_k + T_{jk}, \tag{A4}$$

where

$$T_{jk} = C_{jk} - s_j e_k \tag{A5}$$

contains only the genuine system–environment correlations. By construction, $T_{jk} = 0$ for every factorized initial state, whereas correlated initial states generally satisfy $T_{jk} \neq 0$.

Since both the unitary evolution

$$\rho_{SE}(t) = U(t)\rho_{SE}(0)U^{\dagger}(t)$$

and the partial trace are linear operations, the reduced Bloch vector depends linearly on the correlation tensor T_{jk}.

Evolving $\rho_{SE}(0)$ under $U(t) = e^{-iH_{\mathrm{ex}}t}$ and tracing out E yields

$$\vec{s}(t) = \vec{s}_{\mathrm{pswap}}(t) + \vec{\delta}(t), \tag{A6}$$

where $\vec{s}_{\mathrm{pswap}}(t)$ is the partial-swap expression in Equation (A1) (coming from the $s_j e_k$ part), and

$$\delta_j(t) = \sum_{k,\ell} K_{jk\ell}(t)\,T_{k\ell}, \tag{A7}$$

for some real coefficients $K_{jk\ell}(t)$ determined by H_{ex}.

Equation (A7) makes the physical origin of the deviation explicit: the correction $\vec{\delta}(t)$ is entirely generated by the correlation tensor. When $T_{jk} = 0$, corresponding to an initially factorized state, the deviation vanishes identically and the reduced dynamics reduce exactly to the partial-SWAP expression (A1). Conversely, whenever $T_{jk} \neq 0$, the reduced trajectory generally departs from the partial-SWAP family and cannot, in general, be reproduced simply by varying the unknown environment Bloch vector.

Our witness is precisely sensitive to such deviations: if for some time t^* the measured $z(t^*) = s_z(t^*)$ lies outside the factorized envelope derived from Equation (A1), then necessarily $T \neq 0$, and the initial state $\rho_{SE}(0)$ cannot be written as a product.

Thus, the factorized envelope derived in the main text may be viewed as the set of all trajectories generated under the constraint $T_{jk} = 0$. Any experimentally observed violation of this envelope demonstrates that a nonzero correlation tensor is required to explain the measured dynamics, thereby providing a direct certification of initial system–environment correlations using only the single observable $z(t)$.

References

1. Breuer, H.P.; Petruccione, F. *The Theory of Open Quantum Systems*; Oxford University Press: Oxford, UK, 2002.
2. Alicki, R.; Lendi, K. *Quantum Dynamical Semigroups and Applications*; Springer: Berlin/Heidelberg, Germany, 2007.
3. Pechukas, P. Reduced dynamics need not be completely positive. *Phys. Rev. Lett.* **1994**, *73*, 1060–1062. [CrossRef] [PubMed]
4. Alicki, R. Comment on "Reduced dynamics need not be completely positive". *Phys. Rev. Lett.* **1995**, *75*, 3020. [CrossRef] [PubMed]
5. Shaji, A.; Sudarshan, E.C.G. Who's afraid of not completely positive maps? *Phys. Lett. A* **2005**, *341*, 48–54. [CrossRef]
6. Laine, E.M.; Piilo, J.; Breuer, H.P. Measure for the non-Markovianity of quantum processes. *Phys. Rev. A* **2010**, *81*, 062115. [CrossRef]
7. Modi, K.; Brodutch, A.; Cable, H.; Paterek, T.; Vedral, V. The classical-quantum boundary for correlations: Discord and related measures. *Rev. Mod. Phys.* **2012**, *84*, 1655–1707. [CrossRef]
8. Xie, Y.Y.; Wang, Z.M.; Wu, L.A. Fault-Tolerant Universal Quantum Computing in the Presence of Anisotropic Noise. *arXiv* **2025**, arXiv:2508.04892. [CrossRef]
9. Horodecki, R.; Horodecki, P.; Horodecki, M.; Horodecki, K. Quantum entanglement. *Rev. Mod. Phys.* **2009**, *81*, 865–942. [CrossRef]
10. Ringbauer, M.; Wood, C.J.; Modi, K.; Gilchrist, A.; White, A.G.; Fedrizzi, A. Characterization of memory effects in a quantum environment. *Phys. Rev. Lett.* **2015**, *114*, 090402. [CrossRef] [PubMed]
11. Smirne, A.; Brivio, D.; Cialdi, S.; Vacchini, B.; Paris, M.G. Experimental investigation of memory effects in a decohering quantum system. *Phys. Rev. A* **2011**, *84*, 032112. [CrossRef]
12. Gessner, M.; Breuer, H.P. Detecting nonclassical system-environment correlations by local operations. *Phys. Rev. Lett.* **2011**, *107*, 180402. [CrossRef] [PubMed]
13. Dajka, J.; Łuczka, J.; Hänggi, P. Distance between quantum states in the presence of initial qubit-environment correlations: A comparative study. *Phys. Rev. A* **2011**, *84*, 032120. [CrossRef]
14. Wißmann, S.; Breuer, H.-P.; Vacchini, B. Generalized trace-distance measure connecting quantum and classical non-Markovianity. *Phys. Rev. A* **2013**, *88*, 042108. [CrossRef]
15. Li, C.F.; Tang, J.S.; Li, Y.L.; Guo, G.C. Experimentally accessing the information flow between a system and its environment. *Phys. Rev. A* **2011**, *83*, 064102. [CrossRef]
16. Gessner, M.; Ramm, M.; Pruttivarasin, T.; Buchleitner, A.; Breuer, H.-P.; Häffner, H. Local detection of quantum correlations with a single trapped ion *Nat. Phys.* **2014**, *10*, 105–109. [CrossRef]
17. Chitambar, E.; Abu-Nada, A.; Ceballos, R.; Byrd, M. Restrictions on initial system-environment correlations based on the dynamics of an open quantum system. *Phys. Rev. Lett.* **2015**, *92*, 052110. [CrossRef]
18. Byrd, M.S.; Shu, F.W.; Chitambar, E. System-environment correlations and non-completely positive maps. *Phys. Rev. A* **2016**, *93*, 052101.
19. Sargolzahi, I. Initial correlations in open quantum systems are always detectable. *Phys. Rev. A* **2024**, *109*, 022213. [CrossRef]
20. Zhu, G.; Qu, D.; Xiao, L.; Xue, P. Experimental Detection of Initial System–Environment Entanglement in Open Systems. *Photonics* **2022**, *9*, 883. [CrossRef]
21. Amico, L.; Fazio, R.; Osterloh, A.; Vedral, V. Entanglement in many-body systems. *Rev. Mod. Phys.* **2008**, *80*, 517–576. [CrossRef]
22. Vandersypen, L.M.K.; Chuang, I.L. NMR techniques for quantum control and computation. *Rev. Mod. Phys.* **2005**, *76*, 1037–1069. [CrossRef]

23. Hagen, O.; Byrd, M.S. Tomography-free witnesses of initial system-environment correlations. *Phys. Rev. A* **2021**, *104*, 042406. [CrossRef]
24. Alodjants, A.; Zacharenko, P.; Tsarev, D.; Avdyushina, A.; Nikitina, M.; Khrennikov, A.; Boukhanovsky, A. Random Lasers as Social Processes Simulators. *Entropy* **2023**, *25*, 1601. [CrossRef] [PubMed]
25. Ceballos, R.R. G-Consistent Subsets and Reduced Dynamical Quantum Maps. Ph.D. Thesis, Southern Illinois University, Carbondale, IL, USA, 2017.

Disclaimer/Publisher's Note: The statements, opinions and data contained in all publications are solely those of the individual author(s) and contributor(s) and not of MDPI and/or the editor(s). MDPI and/or the editor(s) disclaim responsibility for any injury to people or property resulting from any ideas, methods, instructions or products referred to in the content.